Effect of MnO$_2$ modification on electrochemical performance of LiNi$_{0.2}$Li$_{0.2}$Mn$_{0.6}$O$_2$ layered solid solution cathode

Yunjian Liu [a,b,c,*], Sanbing Liu [b], Yaping Wang [a], Long Chen [c], Xiaohua Chen [b]

[a] School of Material Science and Technology, Jiangsu University, Zhenjiang, China
[b] Postdoctoral workstation of Chery Automobile Co., Ltd, Wuhu, Anhui, China
[c] School of Automobile and Traffic Engineering, Jiangsu University, Zhenjiang, China

HIGHLIGHTS

► LiNi$_{0.2}$Li$_{0.2}$Mn$_{0.6}$O$_2$ powders are coated by MnO$_2$ with different methods.
► The electrochemical performances of LiNi$_{0.2}$Li$_{0.2}$Mn$_{0.6}$O$_2$ are improved after coating.
► The first coulomb efficiency is increased from 65.9 to 82.7% after MnO$_2$ coating.

ARTICLE INFO

ABSTRACT

Pristine and MnO$_2$-coated LiNi$_{0.2}$Li$_{0.2}$Mn$_{0.6}$O$_2$ powders have been synthesized in this paper. The effect of MnO$_2$ coating on the physical and electrochemical properties is discussed through the characterizations of X-ray diffraction (XRD), scanning electron microscopy (SEM), transmission electron microscopy (TEM), electrochemical impedance spectroscopy (EIS), discharge, cyclic and rate performance tests. The materials show layered structure before and after coating. The MnO$_2$-coated LiNi$_{0.2}$Li$_{0.2}$Mn$_{0.6}$O$_2$ electrodes show better discharge capacity, first coulomb efficiency, cyclic performance and rate capacity compared with pristine LiNi$_{0.2}$Li$_{0.2}$Mn$_{0.6}$O$_2$. And the LiNi$_{0.2}$Li$_{0.2}$Mn$_{0.6}$O$_2$ coated with MnO$_2$ decomposing from manganese carbonate has the best performance. The first coulomb efficiency is 82.7%. The discharge capacities at 0.1 and 10 C are 253 and 99 mAh g^{-1}, respectively, and it presents no obvious capacity loss after 50 cycles. The discharge and cyclic voltammetry (CV) curves show that the coated MnO$_2$ reacts with Li$^+$ during the charge and discharge cycle, which is responsible for higher discharge capacity after coating. Electrochemical impedance spectroscopy (EIS) results show that the R_{ct} of LiNi$_{0.2}$Li$_{0.2}$Mn$_{0.6}$O$_2$ electrode decreases after coating, which is due to the suppression of the solid electrolyte interfacial (SEI) layer development and is responsible for the better cyclic and rate performance.

1. Introduction

Recently, solid solution materials between layered Li[Li$_{1/3}$Mn$_{2/3}$]O$_2$ (commonly designated as Li$_2$MnO$_3$) and LiMO$_2$ (M = Mn, Ni, and Co etc.) [1–3] have been found to be attractive cathodes for lithium-ion batteries as some of them exhibit much higher capacity with lower cost and better safety than the currently used LiCoO$_2$ cathode. The Li$_2$MnO$_3$ component is proposed and demonstrated to stabilize the composite electrode structure, and results in enhancement of the discharge capacity of the electrode by extracting the lithium concomitant with the release of oxygen (a net loss of Li$_2$O) at high potential such as 4.6–4.8 V [4]. For example, the positive electrode Li$_{1.2}$Ni$_{0.2}$Mn$_{0.6}$O$_2$, which can be rewritten in two-component notation as 0.5Li$_2$MnO$_3$·0.5LiNi$_{0.5}$Mn$_{0.5}$O$_2$ ($x = 0.5$), could deliver an initial discharge capacity more than 300 mAh g^{-1} under the above-mentioned conditions [5].

An investigation of the solid solution system has shown that the irreversible capacity (IRC) values of these materials can be as large as 40–100 mAh g^{-1} on charging to 4.8 V depending on the composition [6]. In addition, its poor rate performance should be improved to satisfy the desire for PHEV applications as well as for portable electronic equipment and power tools. Surface modification has been shown to be a facile and useful approach to improve the electrochemical performance of positive electrode materials

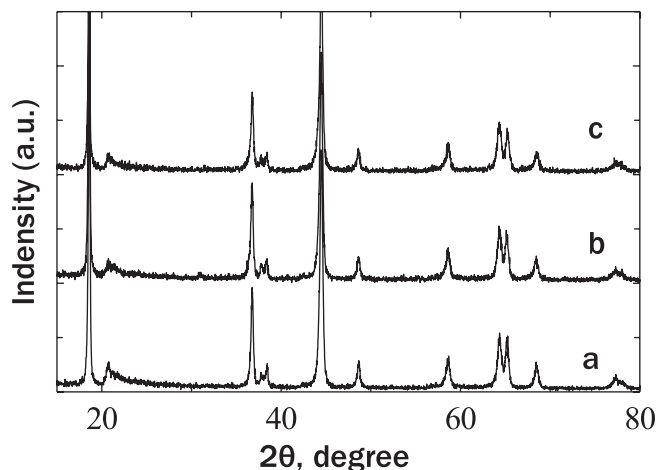**Fig. 1.** XRD patterns of pristine $LiNi_{0.2}Li_{0.2}Mn_{0.6}O_2$ (a), coated by MnO_2 decomposing from manganese hydrate (b) and manganese carbonate (c).

when they are charged to a high cut-off potential. For example, surface-coated layered $Li[Li_{(1-x)/3}Mn_{(2-x)/3}Ni_{x/3}Co_{x/3}]O_2$ electrodes with $Al(OH)_3$, Al_2O_3, CeO_2, ZrO_2, ZnO, $AlPO_4$, TiO_2 and AlF_3 have also been proven to be with lower irreversible capacity loss in comparison with the pristine ones [7–11]. However, the rate capacity of surface-coated layered $Li[Li_{(1-x)/3}Mn_{(2-x)/3}Ni_{x/3}Co_{x/3}]O_2$ electrodes should be improved to satisfy the desire for PHEV applications as well as for portable electronic equipment and power tools. In recently, $LiNiPO_4$ [12] and carbon [13,14] have been reported to enhance the rate capability of high capacity solid solution electrodes.

MnO_2 has been used extensively in electrochemical super-capacitor electrodes [15,16] and graphitic carbons for Li-ion battery [17]. Besides, MnO_2 is a byproduct of Mn dissolution in the $LiMn_2O_4$ electrode, and it is not soluble in the electrolyte [18]. So we just think that MnO_2 should be a new coating material to improve electrochemical properties of pristine materials. $LiLi_{0.2}Ni_{0.2}Mn_{0.6}O_2$ is another promising cathode material for practical application [2,4,19–22]. However, there are few papers focusing on the surface modification of $LiLi_{0.2}Ni_{0.2}Mn_{0.6}O_2$ material. We present here a systematic investigation of surface modification for $LiLi_{0.2}Ni_{0.2}Mn_{0.6}O_2$ by MnO_2 with different processes. The effect of MnO_2 coating on the physical and electrochemical performance has been studied in detail.

2. Experimental

The layered $LiNi_{0.2}Li_{0.2}Mn_{0.6}O_2$ oxide solid solutions were synthesized by a co-precipitation method as previously described [23]. Required amounts of the transition metal acetates were dissolved in deionized water and then added drop by drop into a 0.1 M NaOH solution to form the co-precipitated hydroxides of Mn and Ni, which were then dried overnight at 100 °C in an air-oven, mixed with a required amount of lithium carbonate, heated in air at 500 °C for 4 h and 900 °C for 12 h, then quenched in liquid nitrogen (indicated as 'a').

The surface modification of the synthesized layered oxides was carried out by dispersing the powders in manganese sulfate solution, followed by adding natrium hydroxide or natrium carbonate to precipitate manganese hydroxide or manganese carbonate and heating the products at 400 °C in air for 2 h. So that the MnO_2 content in the final product was controlled to about 5 wt.% (indicated as 'b' and 'c', respectively).

X-ray diffraction (XRD) of these samples was performed on a Panalytical X'Pert diffractometer (Holland) with Cu K_α radiation operated at 40 kV and 30 mA. Data were collected in 2θ range of 10–90° at 2°min^{-1}. The particle size and morphology of the samples were examined by SEM (FEI, Quanta200F) and TEM (Hitachi, 7650).
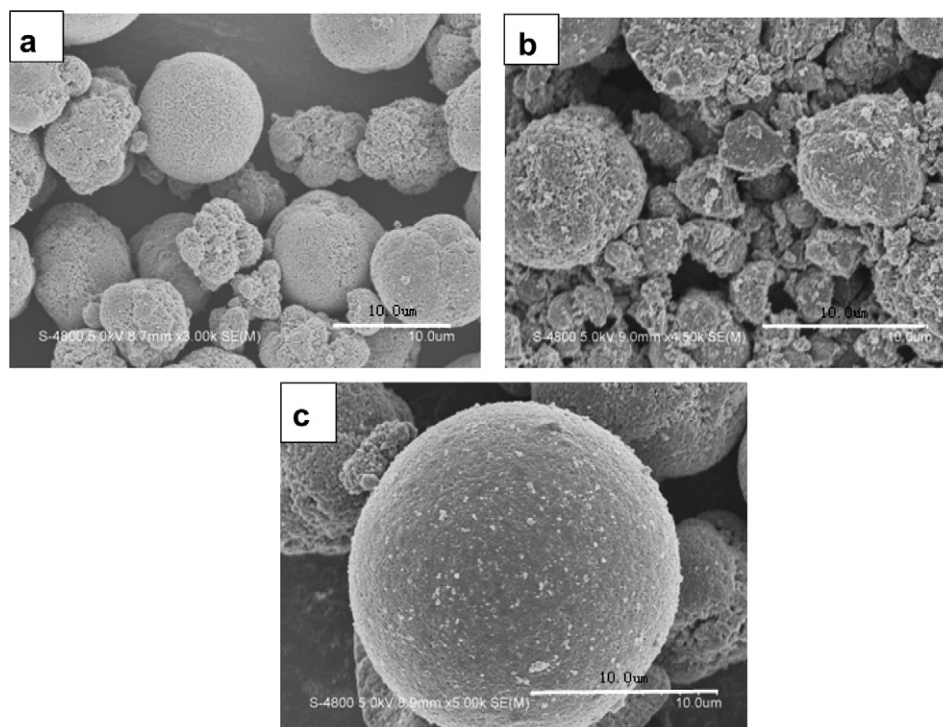

Fig. 2. Scanning electron microscopy (SEM) images of pristine $LiNi_{0.2}Li_{0.2}Mn_{0.6}O_2$ (a), coated by MnO_2 decomposing from manganese hydrate (b) and manganese carbonate (c).

Electrochemical measurements were carried out using R2025 coin-type cells. The positive electrodes were prepared by coating a mixture containing 80% active materials, 10% acetylene black, 10% poly (vinylidene fluoride) binder on circular Al current collector foils followed by drying at 120 °C for 1 h. Electrochemical cells were assembled with the positive electrodes as-prepared, metallic lithium foil as counter electrode, Cellgard 2400 as separator, and 1 M $LiPF_6$ dissolved in ethyl carbonate (EC) and dimethyl carbonate (DMC) (1:1 in volume) as electrolyte in an argon-filled glove box. Charge–discharge experiments were performed galvanostatically with 0.1 C (1 C = 240 mAh g^{-1}) between 2.0 and 4.8 V on battery testers (Land CT2001A).

The cyclic voltammetry (CV) and electrochemical impedance spectroscopy (EIS) of the cells were measured using CHI660A (Chenghua Instrument Co. Ltd, Shanghai) with three electrodes. The amplitude of the AC signal was 5 mV over the frequency range between 100 kHz and 0.01 Hz. The sweep rate of CV was 0.1 mV s^{-1} over a potential of 2.0–5.0 V.

3. Results and discussion

Fig. 1 compares the XRD patterns of bare and MnO_2-coated $LiNi_{0.2}Li_{0.2}Mn_{0.6}O_2$ electrodes. As shown, the as-prepared sample exhibits layered characteristics and all peaks could be indexed on the basis of the α-NaFeO$_2$ structure. Features are present in the 20–25° regions for all samples, indicating the presence of Li$_2$MnO$_3$-type C2/m phase. The results show that the $LiNi_{0.2}Li_{0.2}Mn_{0.6}O_2$

powders remain the layered structure before and after MnO_2 coating.

Fig. 2 shows the scanning electron microscopy (SEM) images of $LiNi_{0.2}Li_{0.2}Mn_{0.6}O_2$ powders before and after coating. The surface of the pristine $LiNi_{0.2}Li_{0.2}Mn_{0.6}O_2$ powders is somewhat smooth. In contrast, the surface of $LiNi_{0.2}Li_{0.2}Mn_{0.6}O_2$ powders becomes considerably rough after coating. It could be distinguished that the MnO_2 coating layer is composed of a large number of nanosized-MnO_2 particles, which distribute independently or connect to each other. Furthermore, the particle size of sample 'b' decreases evidently after surface coating, which should be good to rate performance. The surface areas of sample 'a', 'b' and 'c' are 2.8, 3.8 and 3.4 m^2 g^{-1}, respectively. This is possibly resulted from the cracking of reunited particles during coating process.

Fig. 3 shows TEM images of pristine, MnO_2-coated $Li_{1.2}Ni_{0.2}Mn_{0.6}O_2$ materials. Compared with sample 'a' (Fig. 3(a)), sample 'b' and 'c' particles are coated by MnO_2, as shown in Fig. 3(b) and (c). The partial covering can suppress the side reaction of the active cathode material with electrolyte through reducing their direct contact interface, which favors the cyclic stability.

Fig. 4 shows the initial charge/discharge curves of $LiNi_{0.2}Li_{0.2}Mn_{0.6}O_2$ electrodes before and after coating at the current density of 0.1 C between 2.0 and 4.8 V with constant current–constant voltage (CC–CV) method. The charge process stops when the charge current decreases to 0.01 C. The $LiNi_{0.2}Li_{0.2}Mn_{0.6}O_2$ electrodes can be charged fully with constant current–constant voltage (CC–CV) method. As shown in Fig. 4, all the prepared samples have two distinguished voltage regions during
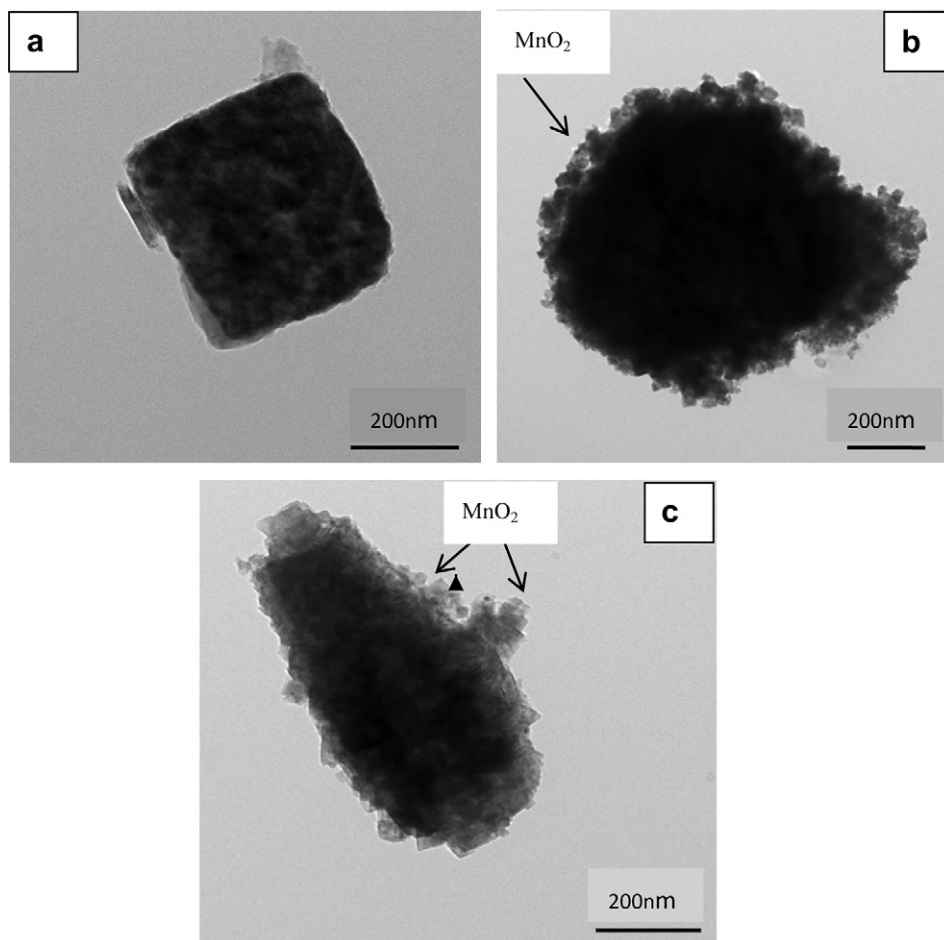

Fig. 3. TEM image of pristine $LiNi_{0.2}Li_{0.2}Mn_{0.6}O_2$ (a), coated by MnO_2 decomposing from manganese hydrate (b) and manganese carbonate (c).
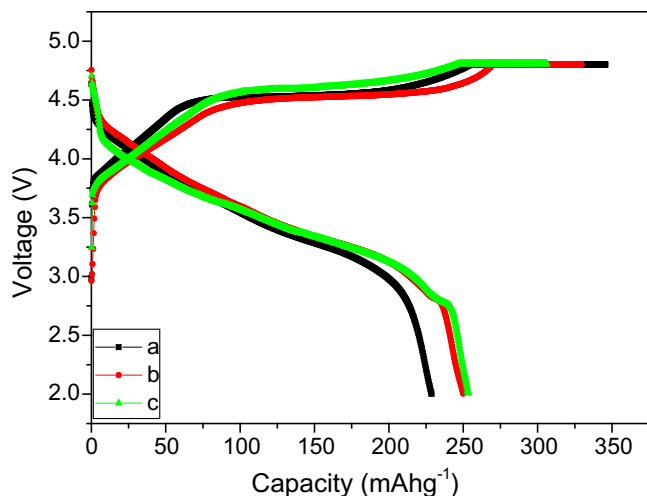
Fig. 4. Charge and discharge curves of pristine $LiNi_{0.2}Li_{0.2}Mn_{0.6}O_2$ (a), coated by MnO_2 decomposing from manganese hydrate (b) and manganese carbonate (c) (0.1 C, 2.0–4.8 V).

Fig. 5. Cyclic performance of pristine $LiNi_{0.2}Li_{0.2}Mn_{0.6}O_2$ and coated electrodes at 0.2 C.

the initial charge process. The appearance of charge plateau at 4.5 V has been caused by the removal of Li_2O from the structure of Li_2MnO_3 [4]. There are plateaus at 4.8 V in the charge curves, which is the constant voltage plateau. Besides, there are small plateaus at 2.8 V in the discharge curves of sample 'b' and 'c'. The results show that the coated MnO_2 on the surface of $LiNi_{0.2}Li_{0.2}Mn_{0.6}O_2$ reacts with Li^+ during the charge and discharge cycles, which should be result in higher discharge capacity. The first discharge capacities of sample 'a', 'b' and 'c' are 228, 250 and 253 mAh g^{-1}, respectively. Table 1 compares the first charge and discharge capacities, IRC values and coulomb efficiencies of $LiNi_{0.2}Li_{0.2}Mn_{0.6}O_2$ materials. As shown in Table 1, the first discharge capacities and coulomb efficiencies of MnO_2-coated samples are higher than that of pristine $LiNi_{0.2}Li_{0.2}Mn_{0.6}O_2$, and the first discharge capacity and coulomb efficiency of $LiNi_{0.2}Li_{0.2}Mn_{0.6}O_2$ coated with MnO_2 decomposing from manganese carbonate are the highest.

As reported in Ref. [8], we are also convinced that the higher discharge capacity and lower IRC of MnO_2-coated material are attributable to a suppression of the reaction between the electrolyte and active material at high potential and an optimization of SEI layer. Another reason for lower IRC of MnO_2-coated material is due to the retention of a more number of oxide ion vacancies in the layered lattice on the surface modification [9]. Besides, during the discharge progress, the coated MnO_2 is inserted with Li^+ and converts to nonstoichiometric $Li_{1+x}Mn_yO_4$ oxides, as shown in the plateau at 2.8 V, which will deliver more discharge capacities. That should be another reason for higher first discharge capacities and coulomb efficiencies of MnO_2-coated $LiNi_{0.2}Li_{0.2}Mn_{0.6}O_2$.

The typical cyclic performances of $LiNi_{0.2}Li_{0.2}Mn_{0.6}O_2$ electrodes cycled at 0.2 C in the voltage range of 2.0–4.8 V are shown in Fig. 5. As can be seen in Fig. 5, it is obviously shown that the cyclic performance is improved significantly by MnO_2 coating. After being

charged/discharged at 0.2 C rate for 50 cycles, the $LiNi_{0.2}Li_{0.2}Mn_{0.6}O_2$ coated with MnO_2 decomposing from manganese hydrate presents a better capacity retention of 94.5% (vs to the first discharge capacity), while the pristine material shows only capacity retention of 91.5%. The $LiNi_{0.2}Li_{0.2}Mn_{0.6}O_2$ coated with MnO_2 decomposing from manganese carbonate presents no obvious capacity loss after 50 cycles. The results show that MnO_2 coating improves the cyclic performance of $LiNi_{0.2}Li_{0.2}Mn_{0.6}O_2$ effectively, and the $LiNi_{0.2}Li_{0.2}Mn_{0.6}O_2$ coated with MnO_2 decomposing from manganese carbonate shows the best results. The MnO_2 coating, which protects $LiNi_{0.2}Li_{0.2}Mn_{0.6}O_2$ electrode from electrolyte attacking, should be responsible for the improved cyclic performance.

Fig. 6 shows the discharge capacities of the $LiNi_{0.2}Li_{0.2}Mn_{0.6}O_2$/Li cells as a function of C-rate between 2.0 and 4.8 V. The cells are charged with a 0.1 C rate before each discharge testing, and then discharged at different C-rates from 0.1 to 10 C rates. As the applied current density increases, all the samples show gradual decreases of discharge capacity. Among the tested samples, the MnO_2-coated $LiNi_{0.2}Li_{0.2}Mn_{0.6}O_2$ electrodes show relatively moderate capacity fade compared with pristine sample as the applied current density increasing. And the $LiNi_{0.2}Li_{0.2}Mn_{0.6}O_2$ coated with MnO_2

Table 1
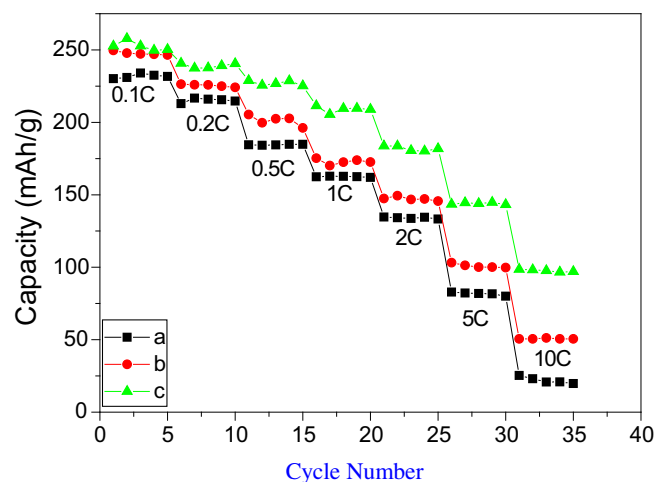Electrochemical cell data collected at 0.1 C rate and 2.0–4.8 V of the layered oxide cathodes.

Samples	Charge capacity (mAh g^{-1})	Discharge capacity (mAh g^{-1})	Irreversible capacity loss (mAh g^{-1})	Coulomb efficiency (%)
a	346	228	118	65.9
b	329	250	79	76.0
c	306	253	53	82.7

Fig. 6. Discharge capacity as a function of C rate for pristine and coated $LiNi_{0.2}Li_{0.2}Mn_{0.6}O_2$ (0.1, 0.2, 0.5, 1, 2, 5 and 10 C).

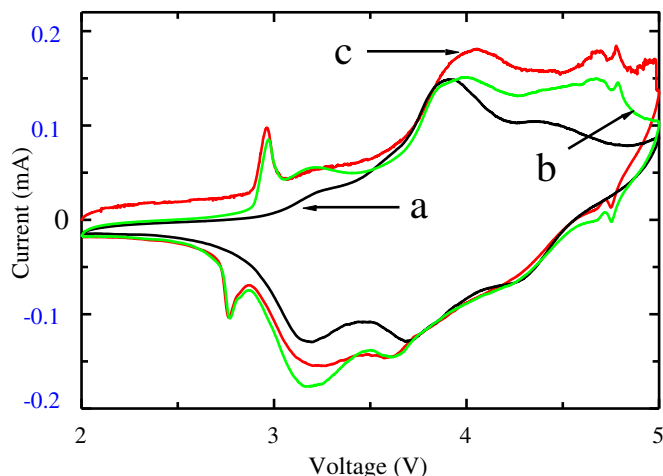**Fig. 7.** CV curves of pristine and coated $LiNi_{0.2}Li_{0.2}Mn_{0.6}O_2$ electrodes (2.0–5.0 V, 0.1 mV s^{-1}).

decomposing from manganese carbonate presents the best rate performance. The discharge capacity of $LiNi_{0.2}Li_{0.2}Mn_{0.6}O_2$ coated with MnO_2 decomposing from manganese carbonate at 10 C is 99 mAh g^{-1}, while that of pristine $LiNi_{0.2}Li_{0.2}Mn_{0.6}O_2$ and $LiNi_{0.2}Li_{0.2}Mn_{0.6}O_2$ coated with MnO_2 decomposing from manganese hydroxide are 25 and 51 mAh g^{-1}, respectively.

Fig. 7 shows the CV curves of synthesized $LiNi_{0.2}Li_{0.2}Mn_{0.6}O_2$ electrodes. As presented in Fig. 7, the redox peaks at about 3.3 V and 3.9 V, which are corresponding to the lithium insertion/extraction reaction from the octahedral site [24], are detected in the curves of synthesized $LiNi_{0.2}Li_{0.2}Mn_{0.6}O_2$ electrodes. But another redox peak at about 2.8 V is found in the curve of MnO_2-coated $LiNi_{0.2}Li_{0.2}Mn_{0.6}O_2$ electrodes. The result is agreed with discharge curves.
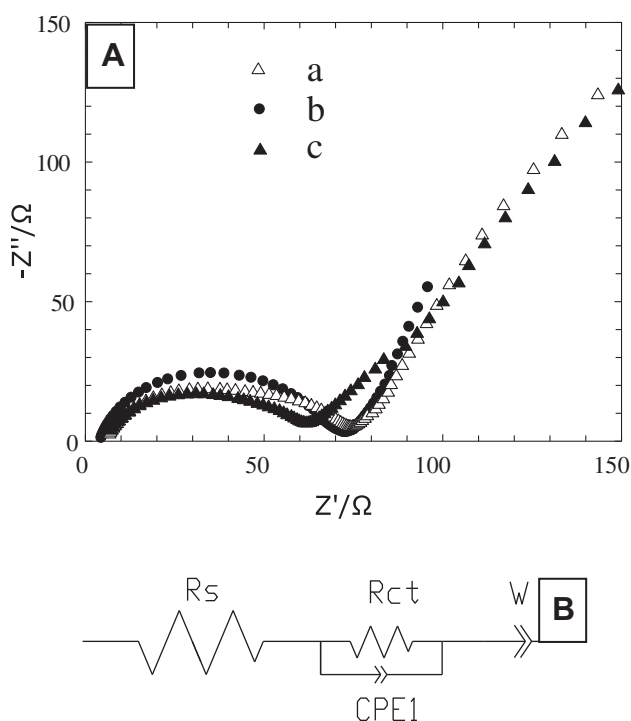

Fig. 8. AC impedance of pristine and coated $LiNi_{0.2}Li_{0.2}Mn_{0.6}O_2$ electrodes (A) and equivalent circuit (B).

Table 2
Impedance parameters of equipment circuit.

Electrodes	R_s (Ω)	R_{ct} (Ω)
a	4.8	68
b	4.3	64
c	4.2	58

The redox peaks at about 2.8 V is associated with the coated MnO_2 inserted with Li$^+$ and converting to nonstoichiometric $Li_{1+x}Mn_yO_4$ oxides. Besides, the redox current of MnO_2-coated $LiNi_{0.2}Li_{0.2}Mn_{0.6}O_2$ is larger than that of pristine sample. The results indicate that the electrical conductivity of MnO_2-coated $LiNi_{0.2}Li_{0.2}Mn_{0.6}O_2$ is larger than that of pristine $LiNi_{0.2}Li_{0.2}Mn_{0.6}O_2$.

Electrochemical impedance spectroscopy (EIS) has been performed to get insight about the difference in electrochemical performance of $LiNi_{0.2}Li_{0.2}Mn_{0.6}O_2$ and MnO_2-coated $LiNi_{0.2}Li_{0.2}Mn_{0.6}O_2$. The measurements are carried out in the charged state of 4.4 V after 10 cycles tested at 0.1 C. The measured impedance spectra are presented in Fig. 8A. A high-frequency semicircle and a low-frequency tail are observed. Generally, an intercept at the Z_{real}-axis in high frequency region corresponded to ohmic resistance (R_s). The high-frequency semicircle is related to charge transfer resistance (R_{ct}). The low-frequency tail is associated with Li$^+$ ion diffusion process in the solid phase of electrode. Each impedance spectrum is fitted with suggested equivalent circuit model (Fig. 8B) to give simulation of the ohmic resistance (R_s) and charge transfer resistance (R_{ct}), as summarized in Table 2. As can be seen in Table 2, R_{ct} of sample 'b' and 'c' is greatly reduced compared with that of pristine electrode. The surface coating decreases R_{ct} by reducing the SEI layer thickness due to a suppressed interaction between the cathode surface and electrolyte while maintaining a micro-porous structure allowing lithium-ions to diffuse through [13]. The higher redox current, lower R_{ct} and bigger surface area are responsible for the better rate performance of $LiNi_{0.2}Li_{0.2}Mn_{0.6}O_2$ after MnO_2 coating.

4. Conclusion

$LiNi_{0.2}Li_{0.2}Mn_{0.6}O_2$ powders are synthesized by co-precipitation method and coated with MnO_2 decomposing from manganese hydrate and manganese carbonate in this paper. The first discharge capacity, coulomb efficiency, cyclic performance and rate capacity of MnO_2 coated $LiNi_{0.2}Li_{0.2}Mn_{0.6}O_2$ are improved compared with pristine $LiNi_{0.2}Li_{0.2}Mn_{0.6}O_2$. The $LiNi_{0.2}Li_{0.2}Mn_{0.6}O_2$ coated with MnO_2 decomposing from manganese carbonate shows the best electrochemical performance. The first discharge capacity and coulomb efficiency are 253 mAh g^{-1} and 82.7%, and it presents no obvious capacity loss after 50 cycles. To be compared, the first discharge capacity and coulomb efficiency of pristine $LiNi_{0.2}Li_{0.2}Mn_{0.6}O_2$ are 228 mAh g^{-1} and 65.9%, and the capacity retention is 91.5%. The discharge capacity of pristine $LiNi_{0.2}Li_{0.2}Mn_{0.6}O_2$ at 10 C rates is increased from 25 to 99 mAh g^{-1} after MnO_2 coating. EIS results show that the R_{ct} of pristine $LiNi_{0.2}Li_{0.2}Mn_{0.6}O_2$ electrode after 10 cycles is decreased after MnO_2 coating, which is due to the suppression of solid electrolyte interfacial (SEI) layer development and responsible for better cyclic and rate performance.

References

[1] D.H. Kim, S.H. Kang, M. Balasubramanian, C.S. Johnson, Electrochem. Commun. 12 (2010) 1618–1621.

[2] F. Wu, H.Q. Lu, Y.F. Su, N. Li, L.Y. Bao, S. Chen, J. Appl. Electrochem. 40 (2010) 783–789.

[3] J.G. Wen, J. Bareno, C.H. Lei, S.H. Kang, M. Balasubramanian, I. Petrov, D.P. Abraham, Solid State Ionics 182 (2011) 98–107.

[4] A.R. Armstrong, M. Holzapfel, P. Novak, C.S. Johnson, S.H. Kang, M.M. Thackeray, P.G. Bruce, J. Am. Chem. Soc. 128 (2006) 8694–8698.

[5] T. Ohzuku, M. Nagayama, K. Tsuji, K. Ariyoshi, J. Mater. Chem. 21 (2011) 10179–10188.

[6] J. Gao, J. Kim1, A. Manthiram, Electrochem. Commun. 11 (2009) 84–86.

[7] J.M. Zheng, Z.R. Zhang, X.B. Wu, Z.X. Dong, Z. Zhu, Y. Yang, J. Electrochem Soc. 155 (2008) A775–A782.

[8] Y. Wu, A. Manthiram, Electrochem. Solid State Lett. 9 (2006) A221–A224.

[9] Y. Wu, A. Manthiram, Solid State Ionics 180 (2009) 50–56.

[10] Y.J. Kang, J.H. Kim, S.W. Lee, Y.K. Sun, Electrochem. Acta 50 (2005) 4784–4791.

[11] J.M. Zheng, J. Li, Z.R. Zhang, X.J. Guo, Y. Yang, Solid State Ionics 179 (2008) 1794–1799.

[12] S.H. Kang, M.M. Thackeray, Electrochem. Commun. 11 (2009) 748–751.

[13] J. Liu, Q. Wang, B.R. Jayan, A. Manthiram, Electrochem. Commun. 12 (2010) 750–753.

[14] J.H. Ju, S.W. Cho, S.G. Hwang, S.R. Yun, Y. Lee, H.M. Jeong, M.J. Hwang, K.M. Kim, K.S. Ryu, Electrochem. Acta 56 (2011) 8791–8796.

[15] D.Q. Liu, Q. Wang, L. Qiao, F. Li, D.S. Wang, Z.B. Yang, D.Y. He, J. Mater. Chem. 22 (2012) 483–487.

[16] W.F. Wei, X.W. Cui, W.X. Chen, D.G. Ivey, Chem. Soc. Rev. 40 (2011) 1697–1721.

[17] P. Israel, C.S. Brad, K.R. Vaikunth, C.G. Philip, Electrochem. Commun. 13 (2011) 590–592.

[18] Y.J. Liu, X.H. Li, H.J. Guo, Z.X. Wang, Q.Y. Hu, W.J. Peng, Y. Yang, J. Power Sources 189 (2009) 721–725.

[19] H. Deng, I. Belharouak, Y.K. Sun, J. Mater. Chem. 19 (2009) 4510–4516.

[20] C.H. Lei, J. Bareno, J.G. Wen, I. Petrov, S.H. Kang, D.P. Abraham, J. Power Sources 178 (2008) 422–433.

[21] J.H. Ryu, B.G. Park, S.B. Kim, J. Appl. Electrochem. 39 (2009) 1059–1066.

[22] G.Z. Wei, X. Lu, F.S. Ke, Adv. Mater. 22 (2010) 4364–4367.

[23] Y.J. Liu, L. Chen, Ionics 18 (2012) 649–653.

[24] C.S. Johnson, N.C. Li, C. Lefief, J.T. Vaughey, M.M. Thackeray, Chem. Mater. 20 (2008) 6095–6101.